

## J-Deconvolution Using Maximum Entropy Reconstruction Applied to $^{13}\text{C}$ – $^{13}\text{C}$ Solid-State Cross-Polarization Magic-Angle-Spinning NMR of Proteins

Ingo Scholz, Stefan Jehle, Peter Schmieder, Matthias Hiller, Frank Eisenmenger, Hartmut Oschkinat, and Barth-Jan van Rossum\*

Leibnizinstitut für Molekulare Pharmakologie, Robert-Rössle-Strasse 10, 13125 Berlin, Germany, and Freie Universität Berlin, Takustrasse 3, 14195 Berlin, Germany

Received February 6, 2007; E-mail: brossum@fmp-berlin.de

Solid-state magic-angle-spinning (MAS) NMR spectroscopy has emerged as a versatile tool for structure determination of biological macromolecules, and several examples of protein structures solved using MAS NMR have been presented recently.<sup>1–5</sup> MAS NMR still relies strongly on  $^{13}\text{C}$  detection. Hence,  $^{13}\text{C}$ – $^{13}\text{C}$  scalar couplings can impair both resolution and sensitivity in  $^{13}\text{C}$ -labeled preparations.  $J$ -couplings lead to a splitting of the carbon lines into multiplets or, when not resolved, become manifest in an effective line broadening.  $\text{C}^\alpha$  signals, for example, contain  $J$ -couplings to the  $\text{C}'$  and, if present, the  $\text{C}^\beta$  spins, with coupling constants of  $J_{\text{C}^\alpha\text{C}'}$   $\approx$  55 and  $J_{\text{C}^\alpha\text{C}^\beta}$   $\approx$  35 Hz, respectively.

Various experimental approaches exist for  $J$ -decoupling. The downside of many experimental methods is that they can bring about a penalty in signal-to-noise ratio ( $S/N$ ) that is often intolerable for solid-state NMR of “difficult” biological samples, like membrane proteins.  $J$ -couplings in the indirect dimension ( $t_1$ ), for example, can be eliminated by using so-called “constant-time” delays.<sup>6</sup> However, this method may result in limited sensitivity because of the relaxation that takes place during the constant-time interval. In solids, relaxation processes are generally fast, which renders this method less practical for sensitivity reasons. Another approach relies on the refocusing of  $J$ -couplings by combining band-selective and hard  $180^\circ$ -pulses to selectively suppress couplings between certain groups of spins. This method was first established for liquid-state NMR<sup>7</sup> and later introduced into solid-state NMR.<sup>8</sup> A drawback is that it can only be applied in  $t_1$ . In a different strategy, homonuclear  $J$ -couplings in the direct dimension ( $t_2$ ) may be removed by using an adiabatic pulse train for selective irradiation during acquisition.<sup>9</sup> This method, however, requires dedicated hardware for simultaneous irradiation and detection on the same NMR nucleus. An innovative method that allows  $J$ -decoupling in both dimensions is based on combination of an IPAP spin-state selection filter within a constant-time interval in  $t_1$  with a zero-quantum PDS (proton-driven spin diffusion) sequence, resulting in a spin-state selective polarization transfer.<sup>10,11</sup> The constant time interval and the duration of the selective pulses to ensure spin-state selection, however, may cause a substantial loss in sensitivity owing to relaxation.

An alternative strategy to remove  $J$ -couplings is by postacquisition data processing. Deconvolution of the raw time-domain data using maximum-entropy (MaxEnt) reconstruction to remove  $J$ -couplings has been demonstrated for liquid-state NMR data.<sup>12–15</sup> The purpose of this Communication is to demonstrate that deconvolution of MAS NMR data with MaxEnt reconstruction allows removal of splittings due to  $J$ -couplings without expenses in sensitivity. We show that a combination of MaxEnt reconstruction in  $t_2$  with a selective pulse in  $t_1$  produces fully  $J$ -resolved data in both dimensions. The method was applied to preparations of proteins expressed on media containing  $[2-^{13}\text{C}]$ -glycerol as the only

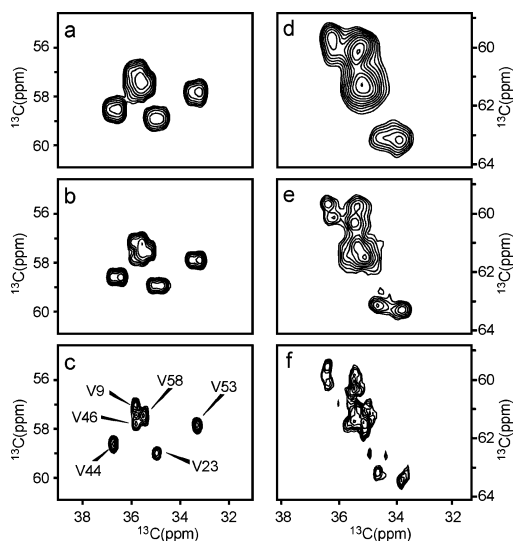


**Figure 1.** Valine  $\text{C}^\alpha$ – $\text{C}^\beta$  cross-peaks of 2-SH3 (a–c) and 2-OmpG (d–f), recorded or processed under different conditions. The data shown in panels a and d are 2D PDS reference spectra (25 ms mixing).<sup>17</sup> The spectra in panels b and e additionally contained a hard  $180^\circ$  pulse and band-selective refocusing pulse on the  $\text{C}^\alpha$ s during  $t_1$ . Panels c and f show the same data as in panels b and e, respectively, deconvoluted with maximum-entropy reconstruction instead of FFT in  $t_2$ , using the Rowland NMR Toolkit version 3.0 ([http://structbio.uhc.edu/hochlab\\_files/rnmrtk.html](http://structbio.uhc.edu/hochlab_files/rnmrtk.html)). The  $J$ -coupling constant for MaxEnt reconstruction was set to 35 Hz. The data on 2-SH3 were recorded on a 9.4 T Avance-400 spectrometer, the spectra on 2-OmpG on a 17.6 T DMX-750 spectrometer (Bruker, Karlsruhe, Germany). For both experiments the MAS frequency was set to 8 kHz. The preparation procedures of OmpG and SH3 were described elsewhere.<sup>16,18</sup> The proteins were expressed in bacteria on media with  $[2-^{13}\text{C}]$ -glycerol<sup>19</sup> as the sole carbon source.

carbon source, leading to labeling schemes that result in a restricted set of  $J$ -couplings so that the effect of decoupling is readily observed. When using  $[2-^{13}\text{C}]$ -glycerol as carbon source, valines contain  $^{13}\text{C}^\alpha$ – $^{13}\text{C}^\beta$  spin-pairs that can be suitably used for investigation of the performance of the decoupling technique without being obscured by overlap from signals from other residues. As a test system we used a  $[2-^{13}\text{C}]$ -glycerol preparation of the  $\alpha$ -spectrin SH3 domain, which is denoted as 2-SH3.<sup>1</sup> As an example of a membrane protein with higher molecular weight (281 residues), we used a preparation of the outer-membrane protein G obtained using  $[2-^{13}\text{C}]$ -glycerol as carbon source, denoted as 2-OmpG.<sup>16</sup>

Figures 1a–c show the valine  $\text{C}^\alpha$ – $\text{C}^\beta$  cross-peaks of 2-SH3, recorded or processed under different conditions. The data in Figure 1a is the reference spectrum, which is a 2D PDS<sup>17</sup> correlation experiment (25 ms mixing). The spectrum in Figure 1b was obtained with similar experimental settings, but the pulse sequence additionally contained a hard  $180^\circ$ -pulse and a band-selective  $180^\circ$ -pulse at the frequency of the  $\text{C}^\alpha$  during  $t_1$ . Figure 1c shows the same

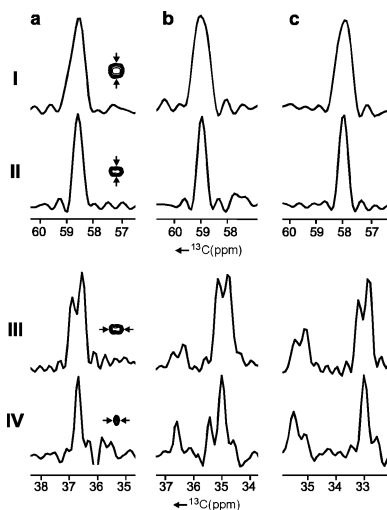


**Figure 2.** Slices extracted from Figure 1 for the SH3  $C^{\alpha}$ – $C^{\beta}$  cross-peak of V44 (a), V23 (b), and V53 (c). The small icons schematically depict the cross-peaks as observed in the 2D data and show the dimension of the extracted slices. Columns extracted from Figure 1a are displayed in panel I; columns and rows taken from Figure 1b are shown in panels II and III, respectively; rows taken from Figure 1c are shown in panel IV.

experiment as in Figure 1b, but processed with MaxEnt deconvolution in  $t_2$ . In Figure 2, we compare various columns and rows extracted from the data in Figure 1a–c. The differences in line widths under free precession and under homonuclear decoupling approximately match with a scalar coupling constant  $J_{C^{\alpha}C^{\beta}}$  of  $\sim 35$  Hz. Hence, even though the  $J$ -couplings are not resolved in the indirect dimension of the experiment, the line widths are reduced by the selective pulses (Figure 2, rows I and II). In the direct dimension, the splittings due to the  $J$ -coupling between the valine  $C^{\alpha}$  and  $C^{\beta}$  spins are partially resolved and collapse into single peaks after performing  $J$ -deconvolution with MaxEnt (Figure 2, rows III and IV, respectively). The  $S/N$  value for the various cross-peaks increases from Figure 1a to Figure 1b (see Supporting Information). It is difficult to compare this to the  $S/N$  in the data reconstructed with MaxEnt (Figure 1c), since the apparent noise can be tuned by the choice of parameters used for the reconstruction. Our aim was to remove the  $J$ -coupling and not the noise, hence we chose the parameters in such a way that the experimental data and the reconstructed data have about the same  $S/N$ .

The results for 2-OmpG are shown in Figures 1d–f. The data in Figure 1d contains the reference spectrum while the spectrum in Figure 1e was recorded using a band-selective refocusing pulse at the  $C^{\alpha}$  frequency during  $t_1$ . Figure 1f shows the same experimental data as in Figure 1e, but processed with MaxEnt deconvolution in  $t_2$ . Without  $J$ -decoupling (Figure 1d), the 2D  $^{13}C$ – $^{13}C$  PDS spectrum is very congested in the valine  $C^{\alpha}$ – $C^{\beta}$  region, which, for OmpG, comprises the response from 14 valine  $C^{\alpha}$ – $C^{\beta}$  cross-peaks. With homonuclear  $J$ -decoupling applied in  $t_1$ , the region of the  $C^{\alpha}$ – $C^{\beta}$  cross-peaks becomes better resolved (Figure 1e). The best resolution is obtained if the data are additionally processed with MaxEnt in  $t_2$  (Figure 1f).

MaxEnt deconvolution needs to be performed carefully to guarantee that the “mock” FID (the product of the inverse Fourier

transform of the reconstructed spectrum with the convolution kernel) closely resembles the experimental FID and differences should be within the error tolerance set for the calculations (see Supporting Information).<sup>12</sup> Possible artefacts that may arise in the reconstructed spectra are ghost signals or phase distortions. To obtain a qualitative estimate about the reliability of the method, we compared data obtained from 2-OmpG deconvolved in  $t_1$  using the MaxEnt reconstruction method with data recorded with experimental  $J$ -decoupling (data shown in the Supporting Information). The experimentally decoupled data shows that the  $t_1$ -line widths are very similar to those obtained by processing with MaxEnt and that differences in the cross-peak positions in  $t_1$  are small ( $\leq 0.2$  ppm).

In conclusion, we have demonstrated that  $J$ -decoupling using refocusing pulses in  $t_1$  and MaxEnt reconstruction in  $t_2$  leads to well-resolved spectra without sacrificing the  $S/N$  to an intolerable amount. Since MaxEnt is a postacquisition processing method, existing data can be reprocessed and analyzed in greater detail. MaxEnt reconstruction can be seen as a powerful and viable alternative to experimental approaches for  $J$ -decoupling.

**Acknowledgment.** Support from the DFG (Grant No.: SFB 449) is gratefully acknowledged.

**Supporting Information Available:** Comparison of  $J$ -decoupled data using experimental and maximum entropy deconvolution, NMR pulse program for  $J$ -decoupling in  $t_1$ , and numeric data of signal-to-noise and line widths. This material is available free of charge via the Internet at <http://pubs.acs.org>.

## References

- Castellani, F.; van Rossum, B.; Diehl, A.; Schubert, M.; Rehbein, K.; Oschkinat, H. *Nature* **2002**, *420*, 98–102.
- Rienstra, C. M.; Hohwy, M.; Mueller, L. J.; Jaroniec, C. P.; Reif, B.; Griffin, R. G. *J. Am. Chem. Soc.* **2002**, *124*, 11908–11922.
- Zech, S. G.; Wand, A. J.; McDermott, A. E. *J. Am. Chem. Soc.* **2005**, *127*, 8618–8626.
- Lange, A.; Giller, K.; Hornig, S.; Martin-Eauclaire, M. F.; Pongs, O.; Becker, S.; Baldus, M. *Nature* **2006**, *440*, 959–962.
- Ritter, C.; Maddelein, M. L.; Siemer, A. B.; Luhrs, T.; Ernst, M.; Meier, B. H.; Sauppe, S. J.; Riek, R. *Nature* **2005**, *435*, 844–848.
- Ernst, R. R.; Bodenhausen, G.; Wokaun, A. *Principles of Nuclear Magnetic Resonance in One and Two Dimensions*; Clarendon Press: Oxford, 2002.
- Bruschweiler, R.; Griesinger, C.; Sorensen, O. W.; Ernst, R. R. *J. Magn. Reson.* **1988**, *78*, 178–185.
- Straus, S. K.; Bremi, T.; Ernst, R. R. *Chem. Phys. Lett.* **1996**, *262*, 709–715.
- Chevelkov, V.; Chen, Z. J.; Bermel, W.; Reif, B. *J. Magn. Reson.* **2005**, *172*, 56–62.
- Duma, L.; Hediger, S.; Lesage, A.; Emsley, L. *J. Magn. Reson.* **2003**, *164*, 187–195.
- Duma, L.; Hediger, S.; Brutscher, B.; Bockmann, A.; Emsley, L. *J. Am. Chem. Soc.* **2003**, *125*, 11816–11817.
- Hoch, J. C.; Stern, A. S. Maximum entropy reconstruction in NMR: an alternative to DFT. In *NMR Data Processing*; Wiley-Liss: New York, 1996; pp 102–135.
- Shimba, N.; Stern, A. S.; Craik, C. S.; Hoch, J. C.; Dotsch, V. *J. Am. Chem. Soc.* **2003**, *125*, 2382–2383.
- Delsuc, M. A.; Levy, G. C. *J. Magn. Reson.* **1988**, *76*, 306–315.
- Jones, J. A.; Hore, P. J. *J. Magn. Reson.* **1991**, *92*, 276–292.
- Hiller, M.; Krabben, L.; Vinothkumar, K. R.; Castellani, F.; van Rossum, B. J.; Kuhlbrandt, W.; Oschkinat, H. *Chem. Biochem.* **2005**, *6*, 1679–1684.
- Suter, D.; Ernst, R. R. *Phys. Rev. B* **1985**, *32*, 5608–5627.
- Pauli, J.; van Rossum, B.; Forster, H.; de Groot, H. J. M.; Oschkinat, H. *J. Magn. Reson.* **2000**, *143*, 411–416.
- LeMaster, D. M.; Kushlan, D. M. *J. Am. Chem. Soc.* **1996**, *118*, 9255–9264.

JA070849G